"Supplemental Information"

Identification and characterization of PPARα ligands in the hippocampus

Avik Roy[1], Madhuchhanda Kundu[1], Malabendu Jana[1], Rama K. Mishra[2], Yeni Yung[3], Chi-Hao Luan[4], Frank J. Gonzalez[5], Kalipada Pahan[1,6]

[1]Department of Neurological Sciences, Rush University Medical Center, Chicago, IL; [2]Medicinal and Synthetic Chemistry Core, Center for Molecular Innovation and Drug Discovery, Northwestern University, Evanston, IL**;** [3]Research Resources Center, University of Illinois at Chicago, IL; [4]High Throughput Analysis Laboratory and Department of Molecular Biosciences, Northwestern University, Evanston, IL**;** [5]Laboratory of Metabolism, Center for Cancer Research, National Cancer Institute, National Institutes of Health, Bethesda, MD; [6]Division of Research and Development, Jesse Brown Veterans Affairs Medical Center, 820 South Damen Avenue, Chicago, IL

Running title: Hippocampal ligands of PPARα

To whom correspondence should be addressed:
Kalipada Pahan, Ph.D.
Department of Neurological Sciences
Rush University Medical Center
1735 West Harrison St, Suite 310
Chicago, IL 60612
Telephone (312) 563-3592; Fax (312) 563-3571
Email: Kalipada_Pahan@rush.edu

Supplementary Table 1. List of physiologically available possible nuclear ligands of PPARα in brain

Class of Compounds	MW	Biosynthetic process	CAS Number
3-Hydroxy-(2,2)-dimethyl butanoic acid, ethyl ester	160.0	Fatty acid Oxidation	69737-23-1
Thiosemicarbazones	190-200	Unknown	unknown
Thiazoles	220-240	Unknown	unknown
Thiazolidine esters	250-270	Unknown	unknown
Hexadecanamide	255.01	Very long chain Fatty acid β oxidation	629-54-9
9-octadecenamide	281.38	Very long chain Fatty acid β oxidation	301-02-0

Supplementary Table 2. Peak integration statistics of mass spectrometric analyses for HEX and OCT in *Ppara*-null hippocampal neurons infected with lentivirions containing different Ppara constructs.

	Sample Name	Ion, m/z	Peak R.T, minutes	Adjusted peak area	Peak area of Int. Standard	Rel. Abundance (RA)	%RA
HEX	Vector Only	255.01	13.71	17632	916408	0.019240338	1.92
HEX	FL-Ppara	255.01	13.7	23806805	989368	24.06263898	**2406**
HEX	Y314D-Ppara	255.23	13.7	637636	1710699	0.372734186	37.3
HEX	Y464D-Ppara	255.01	13.72	18646	1149966	0.016214392	1.62
HEX	Y314D/Y464D-Ppara	255.17	13.71	6843	575146	0.011897849	1.19
OCT	Vector Only	281.13	14.49	79623	916408	0.086885972	8.69
OCT	FL-Ppara	280.97	14.5	24671057	989368	24.93617845	**2494**
OCT	Y314D-Ppara	281.23	14.51	827358	1710699	0.48363739	48.4
OCT	Y464D-Ppara	281.24	14.49	266871	1149966	0.2320686	23.2
OCT	Y314D/Y464D-Ppara	281.05	14.49	128107	575146	0.222738226	22.3

Ppara-null hippocampal neurons were transduced with lentivirions containing different Ppara constructs for 48 h followed by the affinity purification through GFP column. After that, the eluted fraction was fractionated with chloroform-methanol extraction procedure and the organic phase was analyzed by GCMS. Peaks for Hexadecanamide (HEX) and 9-octadecenamide (OCT) were analyzed and their detailed peak integration statistics were displayed above. Peak area was adjusted with baseline and then normalized with the peak area of the internal standard [2,4-Bis(α,α-dimethylbenzyl)phenol]. The normalized value was shown as the relative abundance and finally presented in a percent scale.

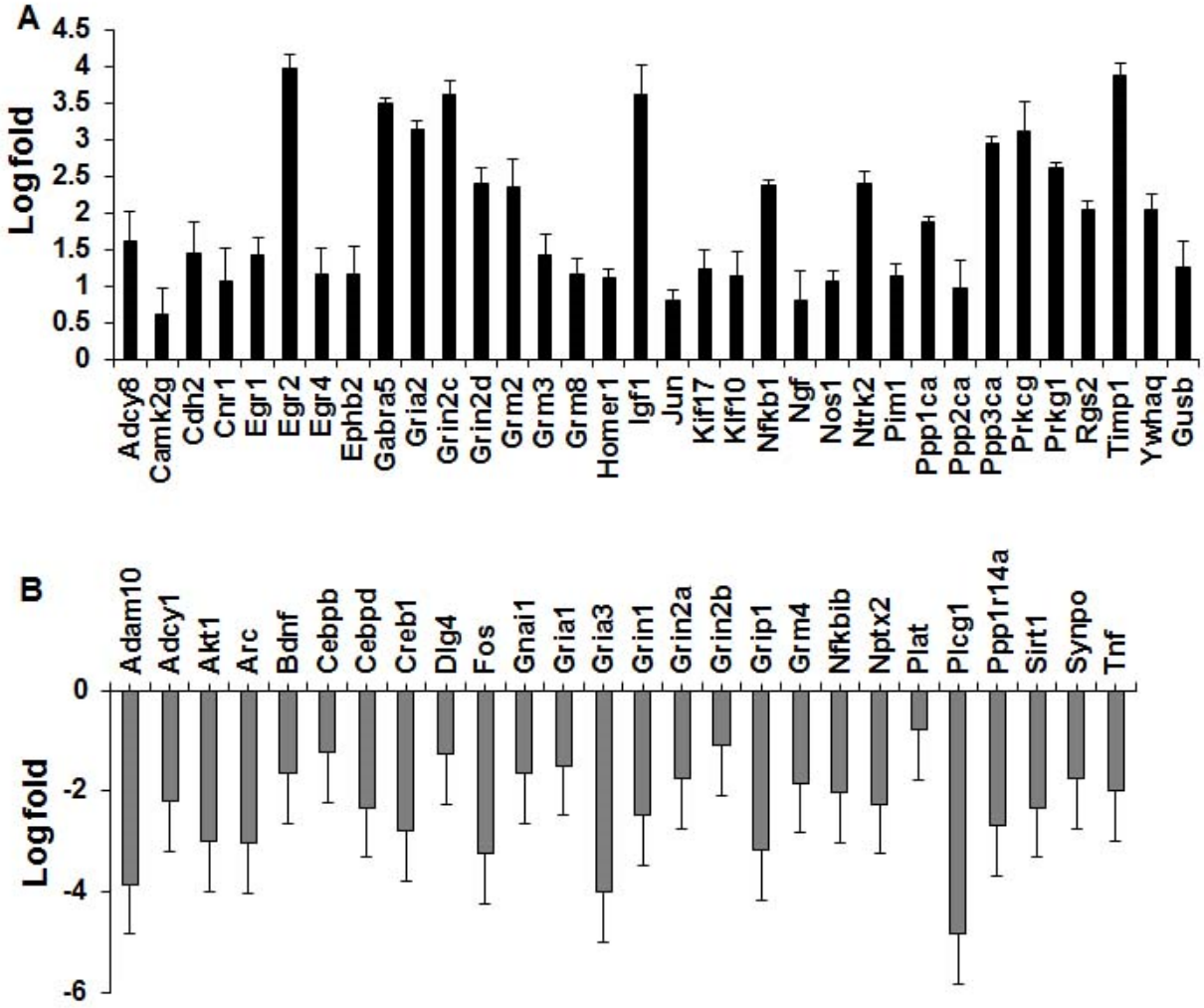

Supplementary Figure 1. Modulation of synaptic molecules in the hippocampus of *Ppara*-null mice. A) Histogram analysis represents the list of upregulated genes in the *Ppara*-null hippocampus as compared to wild type hippocampus plotted as fold change in log scale. B) The list of genes that was down-regulated in the hippocampus of *Ppara*-null mice as compared to wild type mice shown as fold change in log scale. Results are mean $\pm$ SEM of three mice.

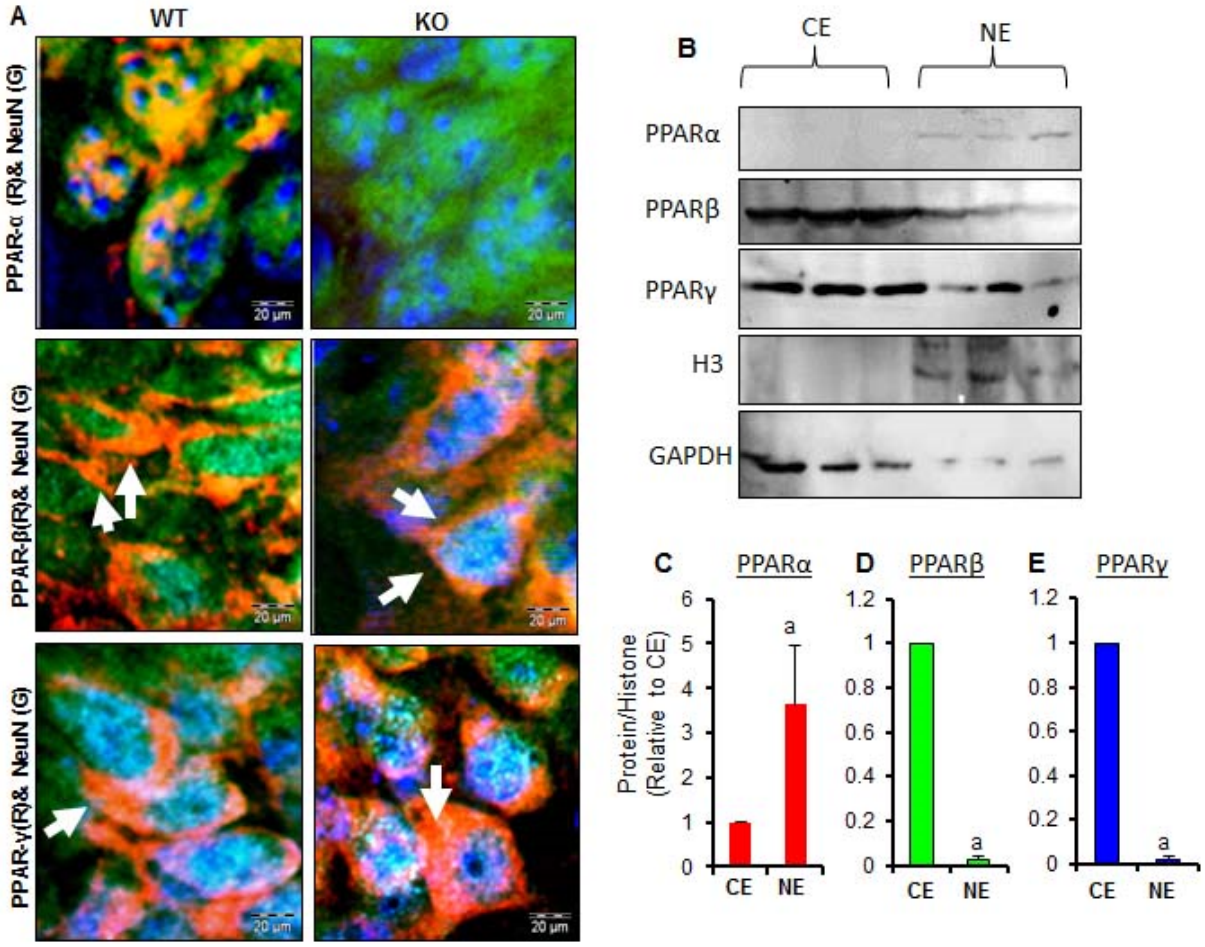

Supplementary Figure 2. The subcellular localization of PPARα, β and γ isotypes in mouse brain hippocampus. (A) The intracellular distribution of PPARα, β and γ were shown by immunofluorescence (NeuN, green; PPARs, red) analyses of the CA1 regions of hippocampus. (B) Nuclear-enriched (NE) and cytoplasmic enriched (CE) fractions of hippocampal tissues were immunoblotted for PPARα, β, and γ. Histone 3 (H3) and GAPDH were included for monitoring purity of nuclear extract and cytoplasmic extract, respectively. Immunoblot analyses were performed in three 6-8 weeks old male WT mice. Bands were scanned and protein/H3 values are presented as relative to CE (C, PPARα; D, PPARβ; E, PPARγ). Results are mean ± SEM of three mice. $^{a}p<0.0001$ *vs CE*.

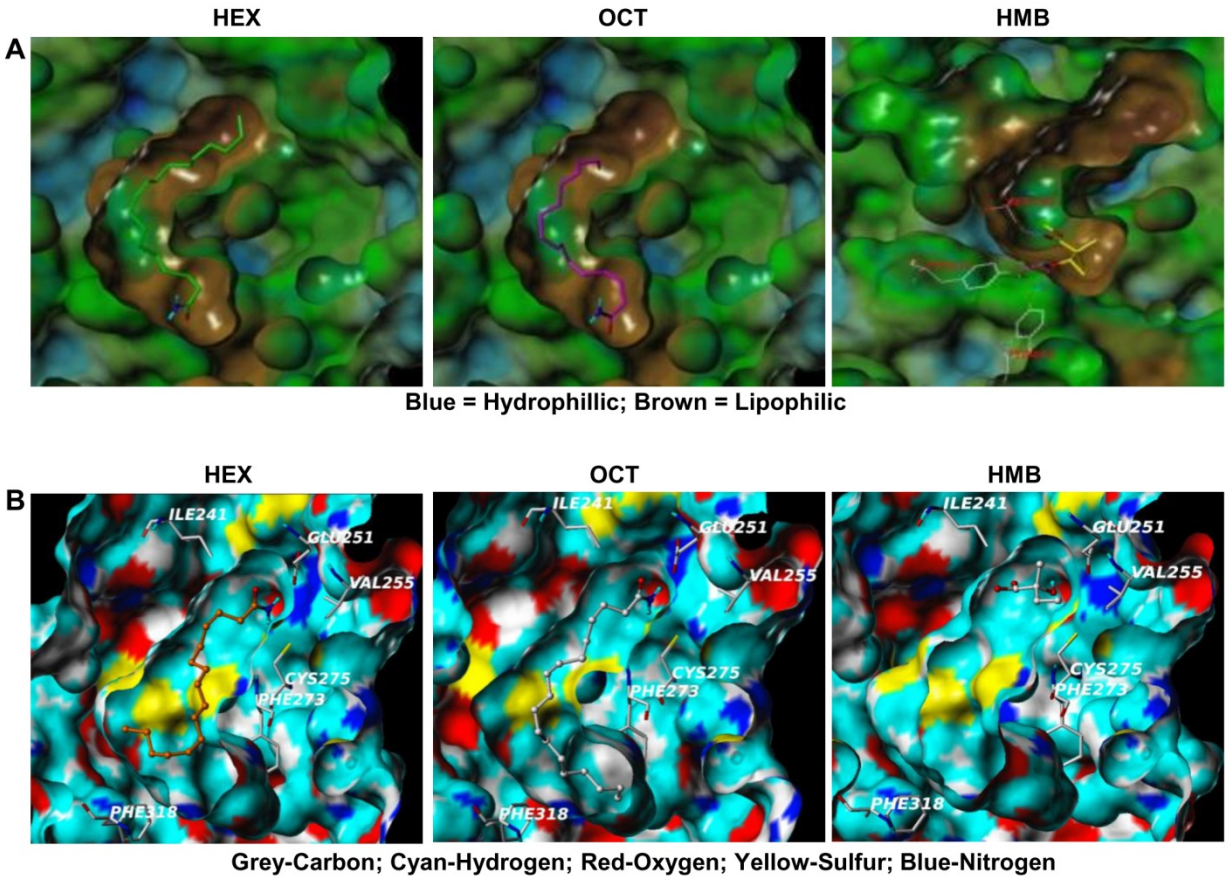

Supplementary Figure 3. Electrostatic potential and atom-specific surfaces of PPARα LBD. (A) Electrostatic potential surface of PPARα LBD docked with HEX (left), OCT (center) and HMB (right). Blue region represents hydrophilic environment, brown for lipophilic surroundings. All three ligands share mostly lipophilic environment (upper panels) with a very few hydrophilic patches). (B) Atom-specific surfaces of PPARα LBD docked with three ligands. (Grey-Carbon; Cyan-Hydrogen; Red-Oxygen; Yellow-Sulfur; Blue-Nitrogen).

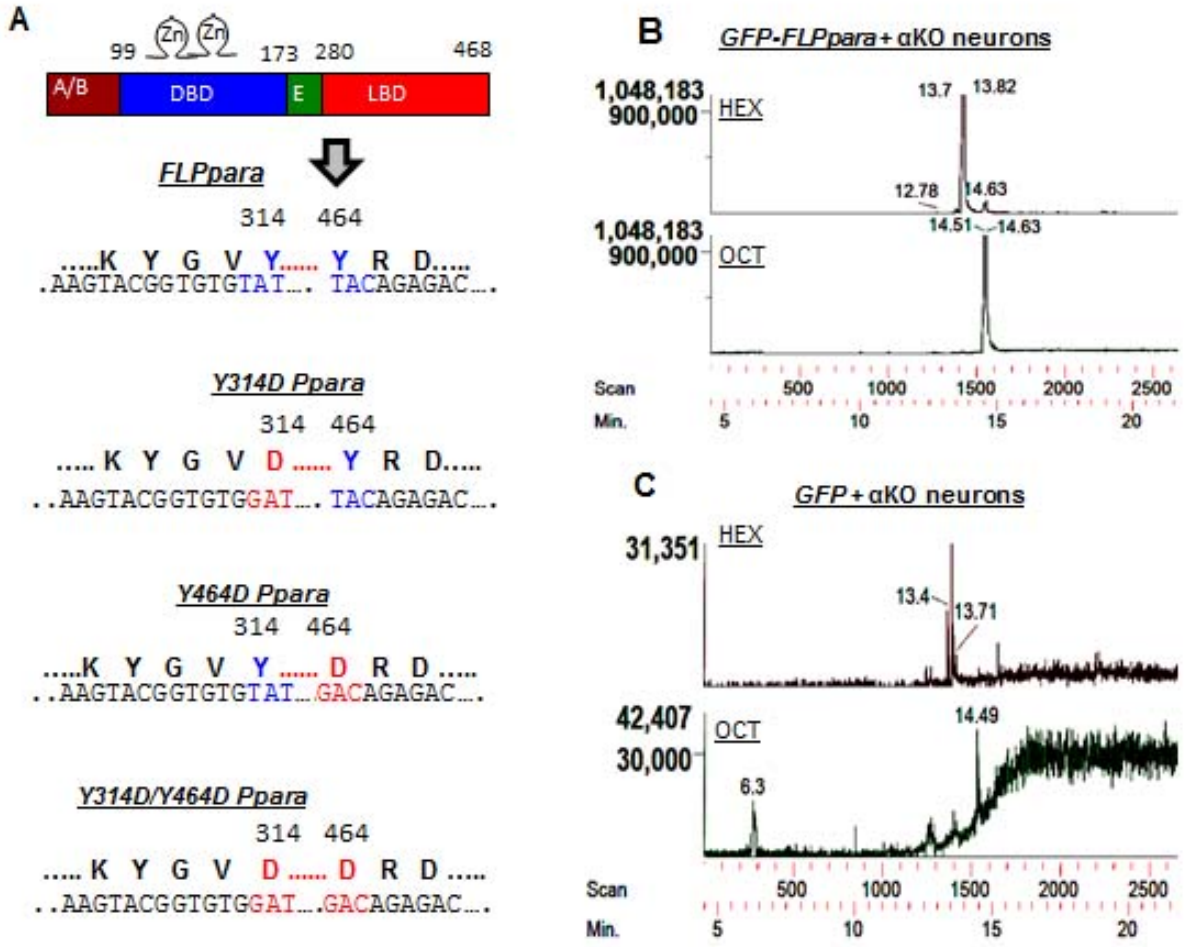

Supplementary Figure 4. Maps of different constructs of PPAR. A) Detailed maps of *FL-Ppara*, *Y314D-Ppara*, *Y464D-Ppara*, and *Y314D/Y464D-Ppara* are shown. GC-MS analyses in GFP-affinity purified extracts of *Ppara*-null hippocampal neurons transduced with lentiviruses containing *GFP-FL-Ppara* (B) and *GFP* (C).

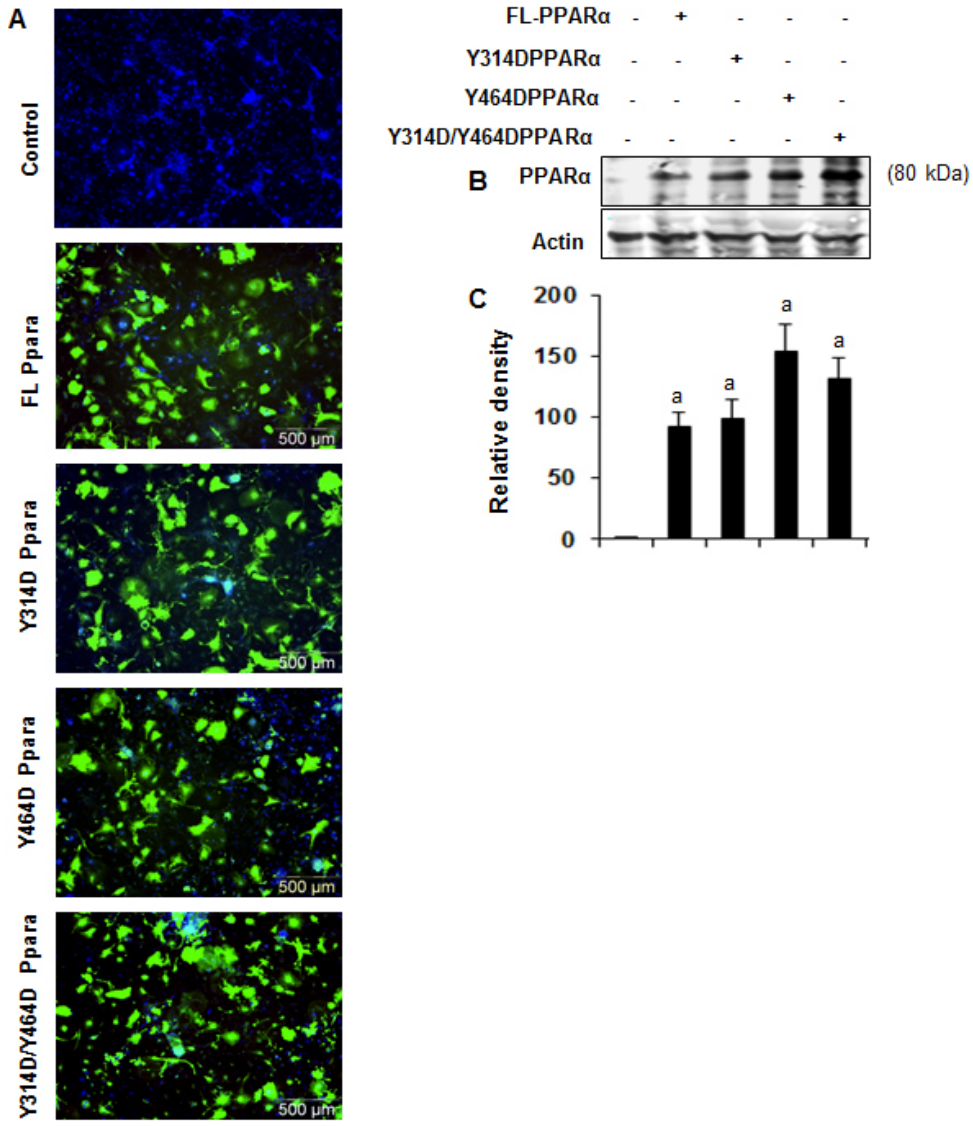

Supplementary Figure 5. Transduction of *Ppara-null* astrocytes with lentiviruses containing different Ppara constructs. A) *Ppara-null* astrocytes cultured on coverslips were transduced with lentiviruses containing *FL-Ppara*, *Y314D-Ppara*, *Y464D-Ppara*, and *Y314D/Y464D-Ppara*. Forty-eight h after transduction, level of GFP was monitored in an Olympus IX81 fluorescence microscope. DAPI was used to visualize nucleus. B) Similarly, 48 h after transduction, the level of PPARα [PPARα (53kDa) + GFP (27 kDa)] was monitored by Western blot. C) Bands were scanned and values (PPARα/Actin) presented as relative to control. Results are mean ± SD of three independent experiments. $^{a}p<0.0001$ *vs control*.

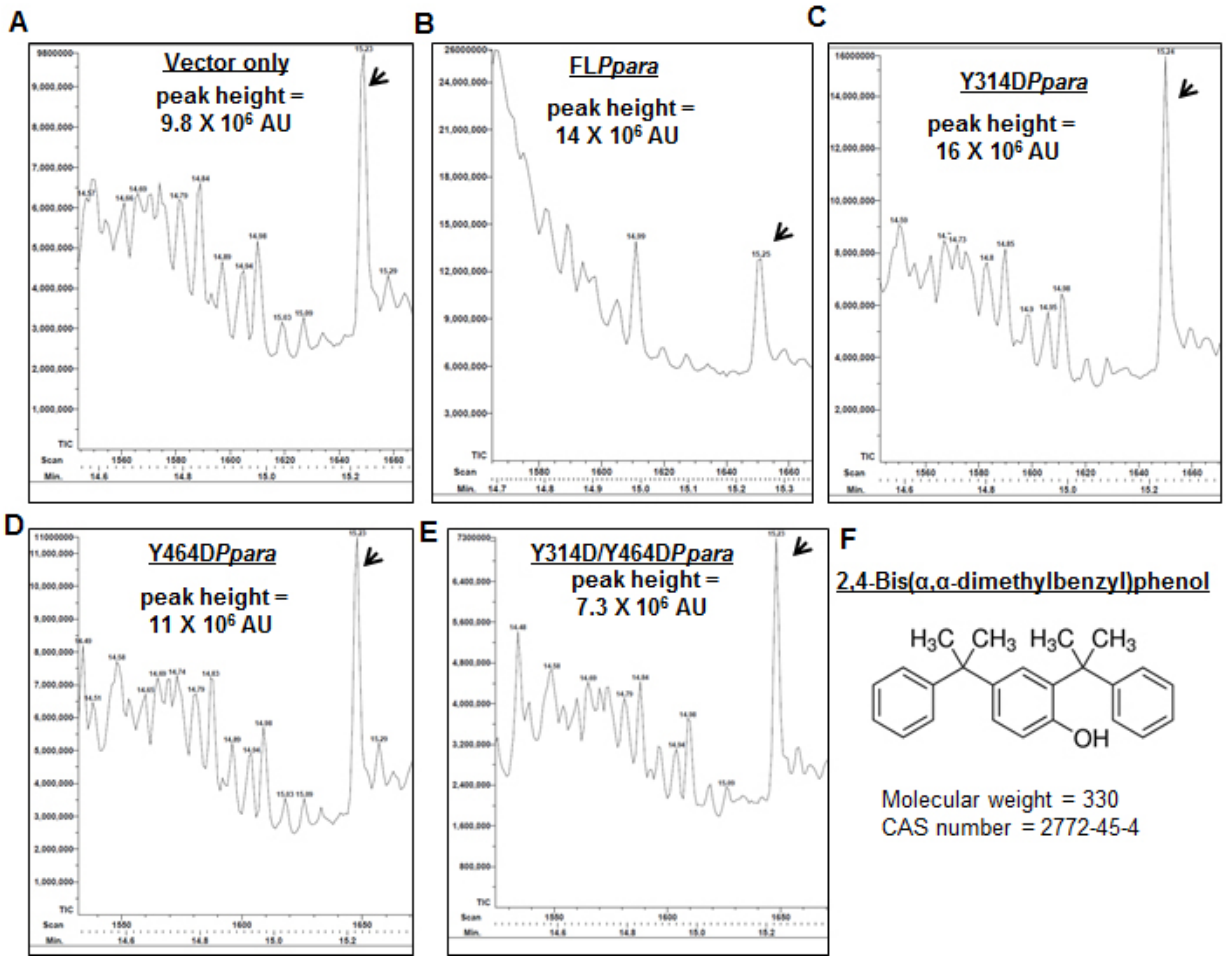

Supplementary Figure 6. Peak integration statistics of GC-MS. 2,4-Bis(α,α-dimethylbenyl)phenol was used as internal standard (arrowhead) in GC-MS analyses (A, vector only; B, *FL-Ppara*; C, *Y314D-Ppara*; D, *Y464D-Ppara*; E, *Y314D/Y464D-Ppara*). F) Chemical structure, molecular weight and CAS number of 2, 4-Bis (α, α-dimethylbenyl) phenol.

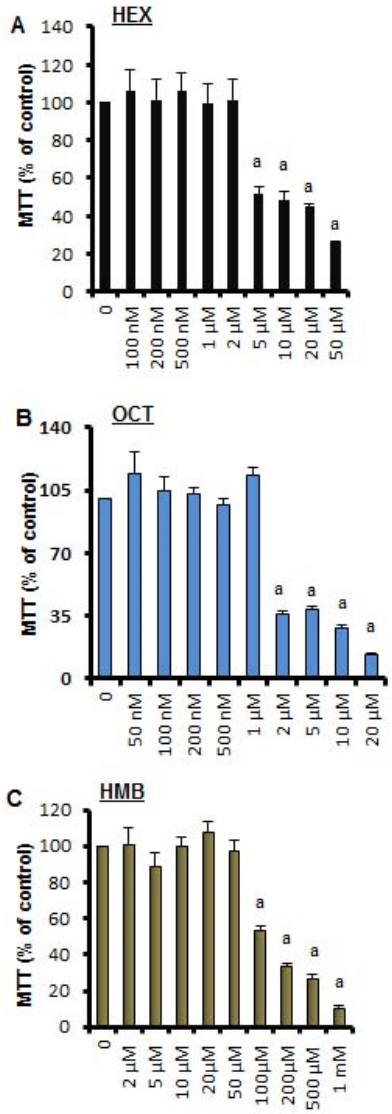

Supplementary Figure 7. Effect of hippocampal ligands of PPARα on the survival of primary mouse astrocytes. Astrocytes plated at 60-70% confluence were transfected with *tk-PPREx3-Luc*, a PPRE-dependent luciferase reporter construct. After 24 h of transfection, cells were treated with different concentrations of HEX (A), OCT (B) and HMB (C) for 4 h followed by monitoring MTT assay to check cell viability. Results are mean ± SD of three independent experiments. $^{a}p< 0.001$ *vs. control.*

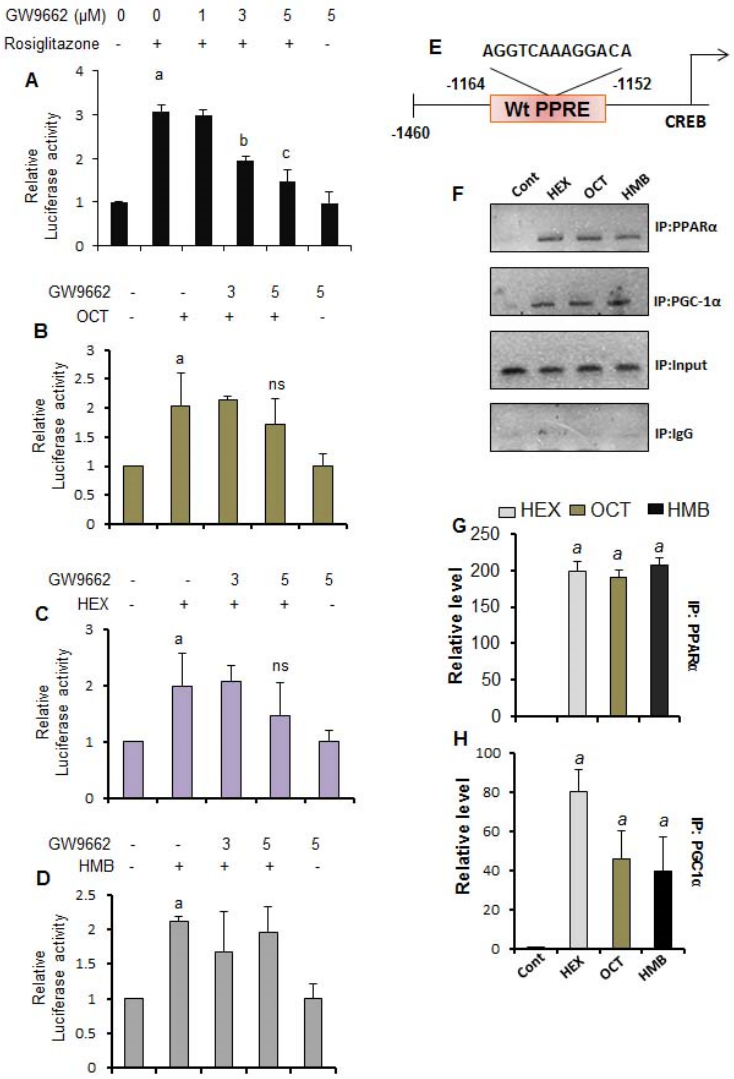

Supplementary Figure 8. OCT, HEX and HMB induce PPRE-driven luciferase activity in *Pparb*-null astrocytes in the presence of PPARγ antagonist. A) *Pparb*-null primary astrocytes plated at 60–70% confluence in 12-well plates were transfected with 0.25 μg of *tkPPREx3-Luc* (a PPRE-dependent luciferase reporter construct). Twenty-four hours after transfection, cells were treated with different concentrations of GW9662 for 30 min followed by stimulation with rosiglitazone. After 4 h, luciferase activities were assayed. Data are mean ± SD of three different experiments. *$^{a}p < 0.001$ versus control; $^{b}p < 0.05$ & $^{c}p < 0.01$ versus rosiglitazone*. After transfection, cells were also treated with GW9662 followed by stimulation with OCT (B), HEX (C) and HMB (D). After 4 h, luciferase activities were assayed. $^{a}p < 0.001$ versus control; ns, not significant. (E) Promoter map of CREB shows the presence of a consensus PPRE. ChIP analyses (F) followed by real-time (G) validation of CREB promoter after pulling down with PPARα and PGC1α. Data are mean ± SD of three different experiments. *$^{a}p < 0.001$ versus control*.

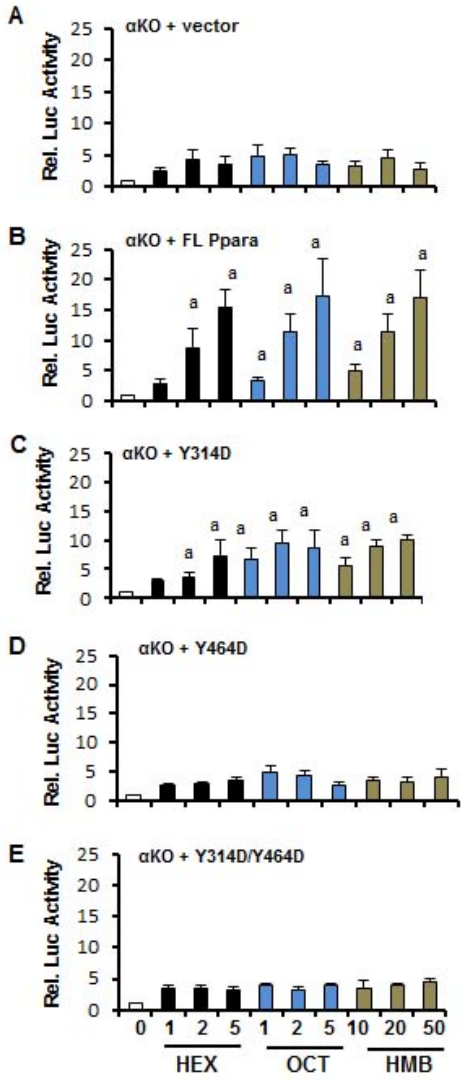

Supplementary Figure 9. Hippocampal ligands of PPARα induce PPRE-driven luciferase activity in primary mouse hippocampal neurons. *Ppara*-null hippocampal neurons were transduced with lentiviruses containing empty vector (A), *FL-Ppara* (B), *Y314D-Ppara* (C), *Y464D-Ppara* (D), and *Y314D/Y464D-Ppara* (E) for 48 h followed by transfection with *tk-PPREx3-Luc*. After 24 h of transfection, cells were treated with different doses of HEX, OCT and HMB for 4 h followed by monitoring luciferase activity. Results are mean ± SD of three independent experiments. $^{a}p< 0.001$ *vs. control.*

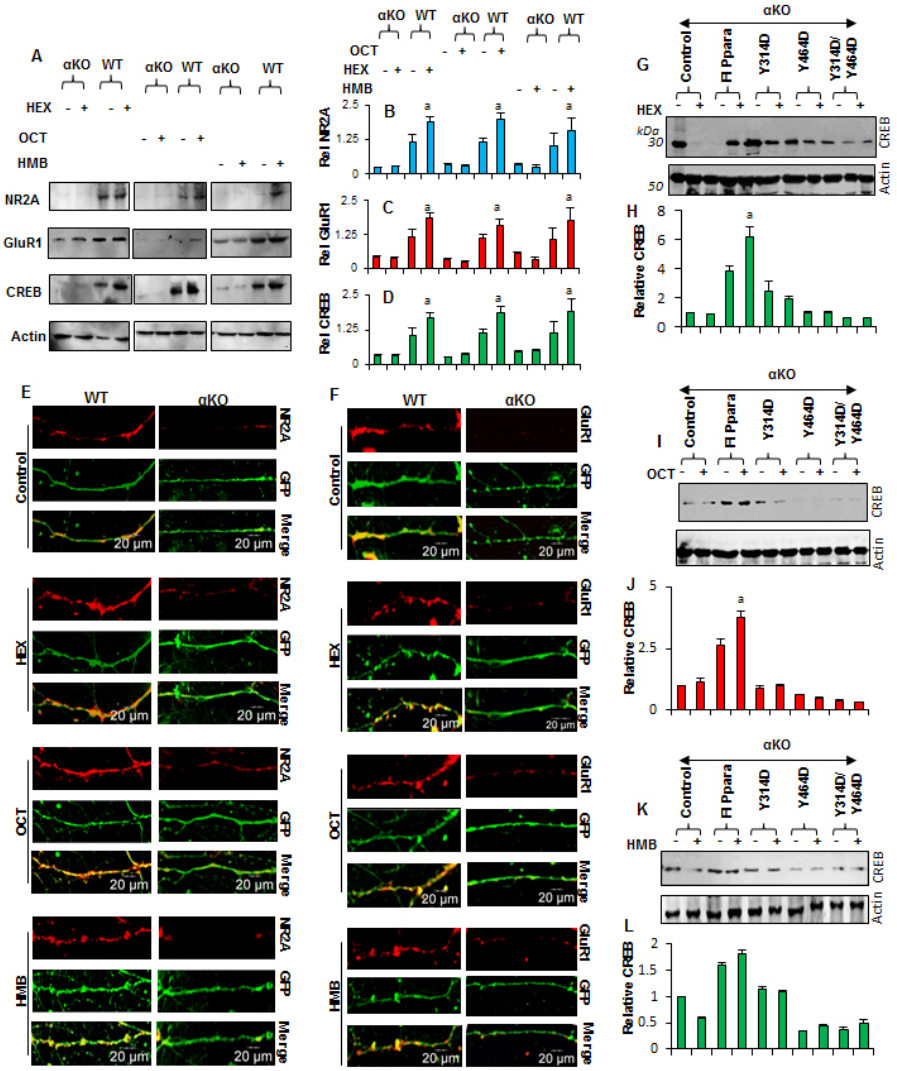

Supplementary Figure 10. Effect of HEX, OCT and HMB on the expression of synaptic molecules in *Ppara*-null hippocampal neurons and neurons transduced with different Ppara constructs. (A) Immunoblot analyses followed by densitometric analyses of NR2A (B), GluR1 (C) and CREB (D) were performed in *Ppara*-null and WT hippocampal neurons treated with 5 μM HEX, 5 μM OCT and 50 μM HMB. Data are mean ± SD of three different experiments. $^{a}p < 0.05$ *versus WT-control*. Immunocytochemical analyses of NR2A (E) and GluR1 (F) in WT and *Ppara*-null hippocampal neurons treated with HEX, OCT and HMB. Hippocampal neurons were transduced with lenti-GFP for 48 h followed by treatment with different ligands. Immunoblot analyses followed by relative densitometric analyses of CREB in *Ppara*-null hippocampal neurons transduced with lentiviruses containing different Ppara constructs followed by treatment with HEX (G-H), OCT (I-J) and HMB (K-L). Bands were scanned and presented as relative to control (H, HEX; J, OCT; L, HMB). Data are mean ± SD of three different experiments. $^{a}p < 0.05$ *vs FL-Ppara control*.

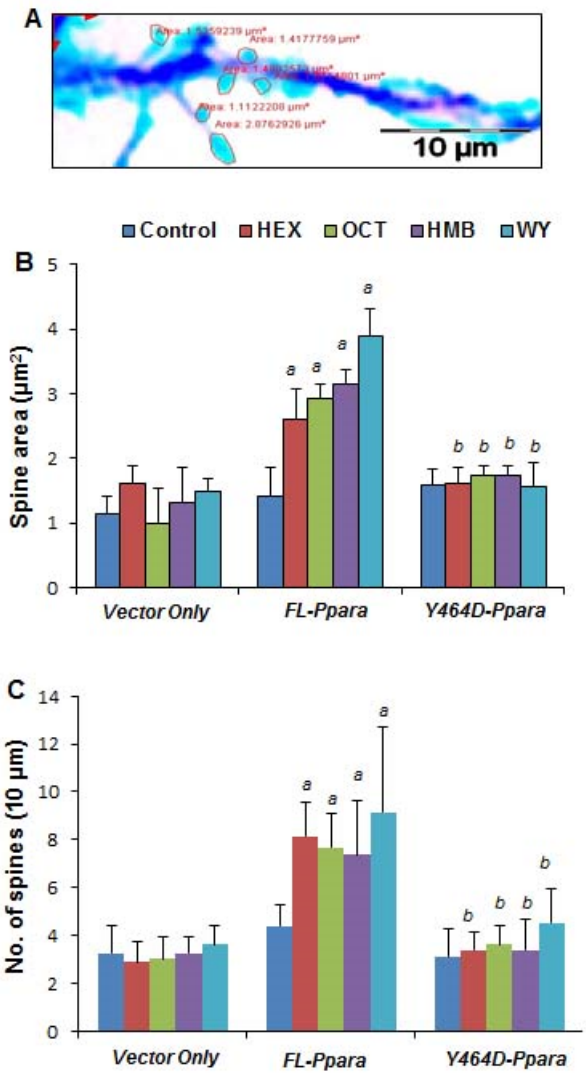

Supplementary Figure 11. Hippocampal ligands of PPARα stimulate morphological plasticity in hippocampal neurons. *Ppara*-null hippocampal neurons were transduced with lentiviruses containing GFP (vector), *FL-Ppara* and *Y464D-Ppara* for 48 h followed by treatment with HEX, OCT, HMB, and WY14643 for 24 h. Then neurons were stained for phalloidin to measure spine density. A) A representative picture of dendrite with spines (Cyan color) used for counting area and number of spines. Area of spine heads (B) and number of spines (C) in 10 µm dendrites were quantified. Results are mean ± SEM of 5 neurons per group. *[a]p<0.05 vs vector only; [b]p<0.05 vs FL-Ppara.*

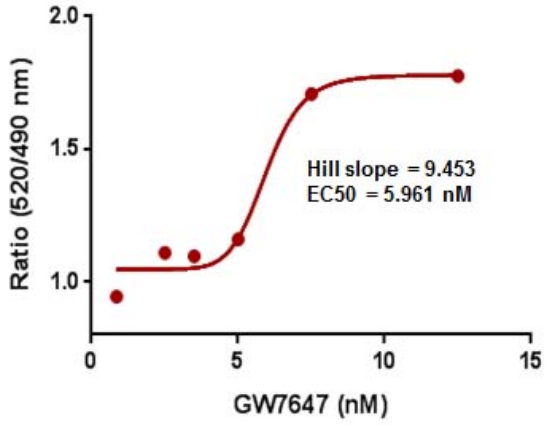

Supplementary Figure 12. Analysis of the interaction of GW7647 with PPARα by TR-FRET. TR-FRET analysis was performed and dose response curves were plotted as a ratio of fluorescence response with increasing doses of agonists. Graph-pad prism 7 software was used to draw a sigmoidal curve-fit. Respective EC50 and hill slope values were calculated based on sigmoidal curve-fit equation, indicated as $Y=Bottom + (X^{Hillslope})*(Top-Bottom)/(X^{Hillslope} + EC50^{Hillslope})$.

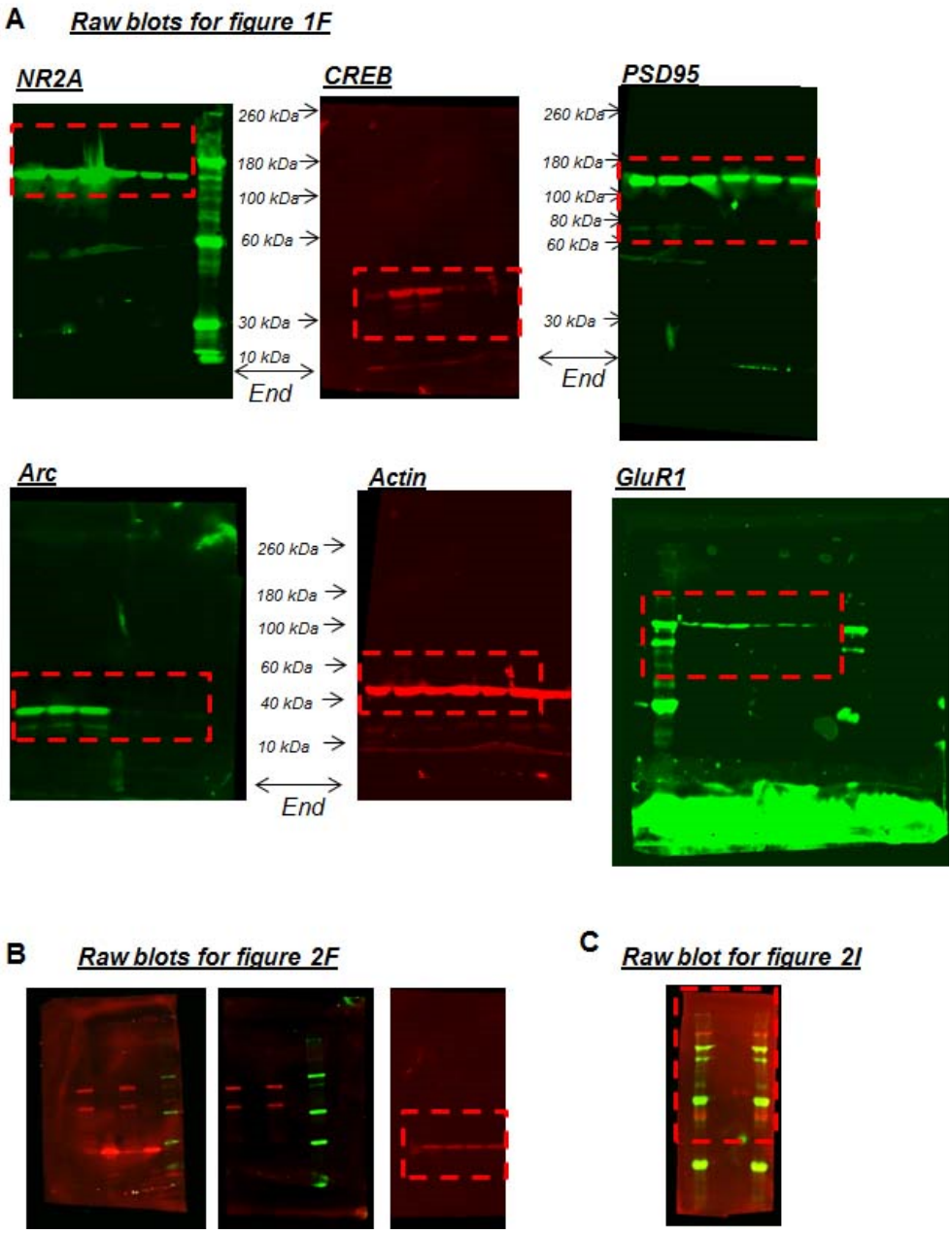

Supplementary Figure 13. Uncut images of Western blots used in main figures. (A, Figure 1H; B, Figure 2F; C, Figure 2I).